may cause unexpected burning of the normal tissues and skin in medical treatment. On the other hand, for the case of the coaxial-slot antenna with choke, the SAR distribution is more localized and more spherical-like, which is more suitable for the interstitial microwave hyperthermia. In addition, the effect on the heating characterization in bio-tissue of the insertion depth of the antenna and the slot width of the choke are also investigated. The results show that the effects are quite small, implying more convenience and lower fabrication limitation can be expected. The fabrication of the antenna is on the way, some experiments will be carried out. In addition, antenna array will be used to obtain a larger heating region to meet the requirements of the big tumor case.

REFERENCES

1. S. Kikuchi, K. Saito, M. Takahashi, and K. Ito, Control of heating pattern for interstitial microwave hyperthermia by a coaxial-dipole antenna—Aiming at treatment of brain tumor, Electron Commun Jpn 90 (2007), 1486–1492.
2. R.D. Nevels, G.D. Arndt, and G.W. Raffoul, Microwave catheter design, IEEE Trans Biomed Eng 45 (1998), 885–890.
3. I. Longo and G.B. Gentili, A coaxial antenna with miniaturized choke for minimally invasive interstitial heating, IEEE Trans Biomed Eng 50 (2003), 82–88.
4. Y. Chang, W. Che, and L. Yang, Thermal distribution analysis in bio-tissues during microwave ablation with FDTD method, In: IEEE Asia Pacific Microwave Conference Dec. 07–11, Singapore, 2009, pp. 1405–1408.
5. K. Saito, A study of the SAR distribution of a coaxial-slot antenna for interstitial microwave hyperthermia by the FDTD method, Electron Commun Jpn 84 (2001), 276–282.
6. W. Che, Y. Chang, L. Yang, L. Yang, and G. Chen, Experimental studies on microwave ablation in vitro animal tissues with microwave percutaneous coagulator, Microwave Opt Technol Lett 50 (2008), 2426–2430.

TRANSMISSION RESONANT FREQUENCY AND ITS AMPLITUDE PREDICTION FOR EBG STRUCTURE BASED ON PHASE COHERENCE

Huansheng Ning,[1] Jun Wang,[1] Wei He,[1] and Lingfeng Mao[2]
[1] School of Electronic and Information Engineering, Beihang University, Beijing, 100191, China; Corresponding author: junwang@ee.buaa.edu.cn
[2] School of Urban Rail Transportation, Soochow University, Suzhou, Jiangsu Province, 215006, China

ABSTRACT: *A new method based on phase coherence is proposed for the strengthened resonant transmission frequency and its amplitude prediction. This method has a clear physical meaning and great convenience. A microstrip electromagnetic bandgap structure is used to verify the method, and both the simulated and measured results demonstrate its validity.* © 2011 Wiley Periodicals, Inc. Microwave Opt Technol Lett 54:409–412, 2012; View this article online at wileyonlinelibrary.com. DOI 10.1002/mop.26570

1. INTRODUCTION

Resonant phenomenon is very common for electromagnetic bandgap (EBG) structures, especially when the structure consists of multiple unit cells, which can be obviously seen in Refs. 1–7. Many researchers have explained this phenomenon with an equivalent circuit model. For instance, the attenuation pole characteristic of defected ground structures can be interpreted by a parallel LC resonator circuit with extracted parameters from the full-wave simulation result. The equivalent circuit method can achieve an accurate prediction of resonant frequencies at relatively low frequencies [8]. However, this method is only applicable for a certain class of EBG structures. But the modeling through a wide range frequency is always difficult because of the stronger electromagnetic behavior at high frequency.

Interference of electromagnetic waves is the combination of separate electromagnetic wave in the same region of space to produce a resultant wave [9]. And the constructive and destructive interferences of two waves occur when phase coherence conditions are satisfied. From this point of view, the transmission resonant phenomenon of EBG structures can be regarded as the constructive and destructive interference of transmitted voltages from each unit cell.

In this article, we propose a simplified model to predict the strengthened transmission resonant frequency and its amplitude of two unit cells based on the characteristic of one unit cell for EBG structure. For the purpose of method verification, one unit cell and two unit cells of a microstrip EBG structure are simulated and fabricated. Both the simulated and measured results demonstrate the method validity. Meanwhile, the reasons for some missed strengthened resonant frequencies in the phase coherence method prediction are also discussed. This proposed method can give a clear physical explanation to the transmission resonance phenomenon and show its great convenience for resonant frequency and its amplitude prediction.

2. TRANSMISSION RESONANT FREQUENCY AND ITS AMPLITUDE PREDICTION METHOD

The characteristic of the unit cell for EBG structure is analyzed as shown in Figure 1(a). Here, the reflected voltage and transmitted voltage are expressed with the aid of transmission coefficient S_{21} and reflection coefficient S_{11} for the unit cell from the viewpoint of scattering matrix [10]. And we assume that the incident power is transmitted along the z-direction. Therefore, the incident
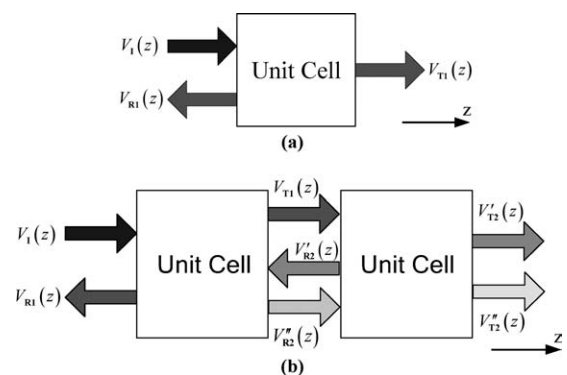
Figure 1 Reflected and transmitted voltages analysis for EBG structure. (a) Characteristic of the unit cell. (b) Transmission resonance analysis for two unit cells

voltage $V_{\mathrm{I}}(z)$, the reflected voltage $V_{\mathrm{R1}}(z)$, and the transmitted voltage $V_{\mathrm{T1}}(z)$ of the unit cell can be written as follows:

$$
\begin{aligned}
V_{\mathrm{I}}(z) &= A_{\mathrm{I}}\exp(-\mathrm{j}\beta z)\\
V_{\mathrm{R1}}(z) &= A_{\mathrm{I}}|S_{11}|\exp[\mathrm{j}(\beta z + \Phi_{11})]\\
V_{\mathrm{T1}}(z) &= A_{\mathrm{I}}|S_{21}|\exp[-\mathrm{j}(\beta z + \Phi_{21})]
\end{aligned}
\qquad (1)
$$

where A_{I} is the amplitude of incident voltage, $|S_{11}|$ and Φ_{11} are the amplitude and phase of S_{11}, $|S_{21}|$ and Φ_{21} are the amplitude and phase of S_{21}.

Henceforth, the transmitted and reflected voltages of two unit cells for EBG structure shown in Figure 1(b) can be obtained as:

$$
\begin{aligned}
V'_{\mathrm{T2}}(z) &= A_{\mathrm{I}}|S_{21}|^2\exp[-\mathrm{j}(\beta z + 2\Phi_{21})]\\
V'_{\mathrm{R2}}(z) &= A_{\mathrm{I}}|S_{21}||S_{11}|\exp[\mathrm{j}(\beta z + \Phi_{21}+\Phi_{11})]\\
V''_{\mathrm{R2}}(z) &= A_{\mathrm{I}}|S_{21}||S_{11}|^2\exp[-\mathrm{j}(\beta z + \Phi_{21}+2\Phi_{11})]\\
V''_{\mathrm{T2}}(z) &= A_{\mathrm{I}}|S_{21}|^2|S_{11}|^2\exp[-\mathrm{j}(\beta z + 2\Phi_{21}+2\Phi_{11})]
\end{aligned}
\qquad (2)
$$

The transmitted voltage $V'_{\mathrm{T2}}(z)$ at the received port is resulted from the direct transmission of the first and second unit cell. The reflected voltage $V'_{\mathrm{R2}}(z)$ is the reflection of $V_{\mathrm{T1}}(z)$ from the second unit and the reflected voltage $V''_{\mathrm{R2}}(z)$ is caused by the reflection of the first unit. The transmitted voltage $V''_{\mathrm{T2}}(z)$ is the transmission of $V''_{\mathrm{R2}}(z)$ through the second unit cell. Thus, the resultant transmitted voltage at the received port is:

$$
\begin{aligned}
V_{\mathrm{R}}(z) &= V'_{\mathrm{T2}}(z) + V''_{\mathrm{T2}}(z)\\
&= A_{\mathrm{I}}|S_{21}|^2\exp[-\mathrm{j}(\beta z + 2\Phi_{21})]\\
&\quad + A_{\mathrm{I}}|S_{21}|^2|S_{11}|^2\exp[-\mathrm{j}(\beta z + 2\Phi_{21}+2\Phi_{11})]\\
&= A_{\mathrm{I}}|S_{21}|^2\exp[-\mathrm{j}(\beta z + 2\Phi_{21})][1 + |S_{11}|^2\exp(2\Phi_{11})]
\end{aligned}
\qquad (3)
$$

Based on the phase coherence condition, the constructive interference of the transmitted voltages, which results in the strengthened resonance of transmission coefficient of two unit cells for EBG structure, occurs at

$$
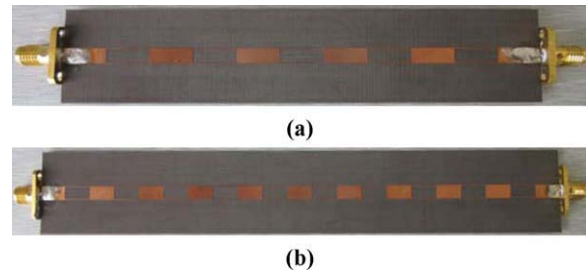\Phi_{11} = n\pi \qquad n = 0, \pm 1, \pm 2, \pm 3 \cdots \qquad (4)
$$

and the amplitude of the transmission coefficient at the strengthened resonant frequency can be approximated by:

$$
(|S'_{21}|)\big|_{f=f_{\mathrm{R}}} = |S_{21}|^2\left(1 + |S_{11}|^2\right) \qquad (5)
$$

where f_{R} is the strengthened transmission resonant frequency.
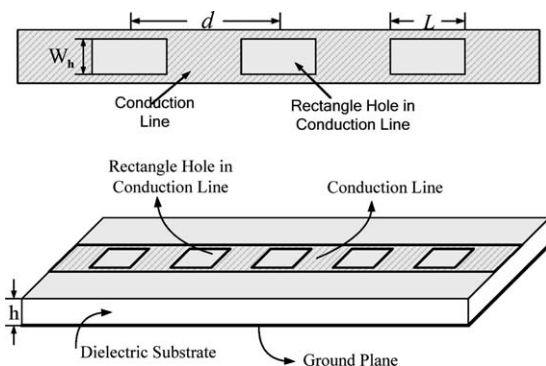
Figure 3 Fabricated microstrip EBG structure. (a) One unit cell. (b) Two unit cells. [Color figure can be viewed in the online issue, which is available at wileyonlinelibrary.com]

From Eq. (4), we can predict the strengthened resonant frequencies for two unit cells from the phase of reflection coefficient of one unit cell. And from Eq. (5), the amplitude of these resonant frequencies can be obtained with transmission coefficient and reflection coefficient for one unit cell. In general, both the strengthened transmission resonant frequency and its amplitude of two unit cells can be predicted with the simulation or measurement of one unit cell for EBG structure.

This method gives a clearer physical explanation to the transmission resonant phenomenon compared with the equivalent circuit modal. In addition, the resonant frequency and its amplitude prediction will provide helpful information for the design and characteristic analysis of EBG structure, which will save much time and computer memory in comparison with the full-wave numerical simulation of the entire structure.

3. METHOD VERIFICATION AND DISCUSSION

A microstrip EBG structure [3] shown in Figure 2, where the periodical rectangle patterns are etched in the conductor line, is used to verify the phase coherence method. The substrate used in the simulation has the parameters as Arlon Cuclad 250(tm), with a thickness $h = 1.50$ mm and dielectric constant of $\varepsilon_{\mathrm{r}} = 2.55$. The width of the 50 Ω microstrip line is set to 4.5 mm. The length and width of the rectangle hole in the conductor line with period $d = 20$ mm are chosen as $W_{\mathrm{h}} = 4$ mm and $L = 10$ mm, respectively.

To achieve an obvious resonant phenomenon, the unit cell of the microstrip EBG structure is composed of five rectangle

Figure 2 Configuration of microstrip EBG structure
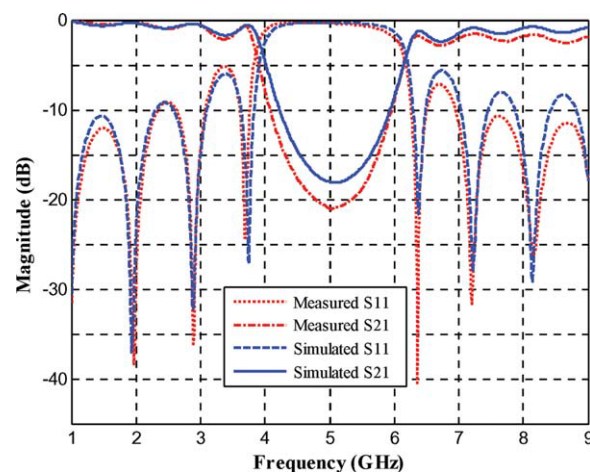
Figure 4 Simulated and measured S-parameters of the unit cell for microstrip EBG structure. [Color figure can be viewed in the online issue, which is available at wileyonlinelibrary.com]
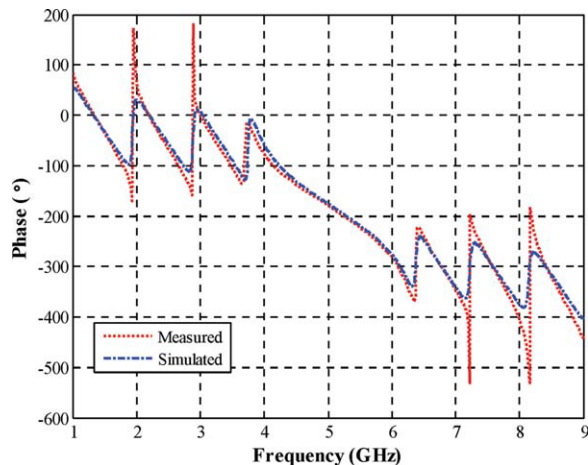
Figure 5 Simulated and measured phase of reflection coefficient for one unit cell. [Color figure can be viewed in the online issue, which is available at wileyonlinelibrary.com]
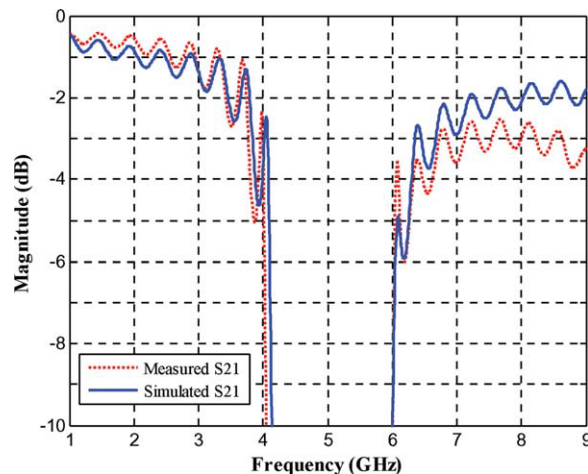
Figure 6 Simulated and measured transmission coefficient for two unit cells of microstrip EBG structure. [Color figure can be viewed in the online issue, which is available at wileyonlinelibrary.com]

holes. And the unit cell is simulated to predict the strengthened transmission resonant frequency and its amplitude for two unit cells. Moreover, the structure including two unit cells is simulated for method verification. Both the unit cell and two unit cells are fabricated and measured to testify the simulation and method analysis.

Figure 3 shows the top view of the fabricated structure, which includes two SMA connectors at both the structure terminations. The good agreement of simulated and measured S-parameters for the unit cell can be seen in Figure 4. And a bandgap with center frequency around 5 GHz is obtained, which is consistent with the Bragg scattering condition. The simulated

and measured phase of reflection coefficient for one unit cell is presented in Figure 5. Although some singular points are introduced in the phase measurement, it does not affect the strengthened transmission resonant frequency prediction. The reason for that is the phase of reflection coefficient at these singular points does not satisfy Eq. (4).

Based on the above simulated and measured results of one unit cell, the strengthened transmission resonant frequency and its amplitude for two unit cells can be predicted. Moreover, the structure composed of two unit cells is simulated and measured for method verification and Figure 6 shows the transmission coefficient results. Tables 1 and 2 give the simulation and mea-

TABLE 1 Simulation Analysis of Strengthened Transmission Resonant Frequency and its Amplitude

Number	Frequency Prediction (GHz)	Magnitude Prediction (dB)	Frequency Simulation (GHz)	Magnitude Simulation (dB)	Frequency Relative Error (%)	Magnitude Deviation (dB)
1	1.32	−0.28	1.44	−0.60	8.33	0.32
2	1.95	−0.34	1.93	−0.74	1.04	0.40
3	2.20	−0.38	2.41	−0.84	8.71	0.46
4	2.91	−0.42	2.88	−0.93	1.04	0.51
5	3.03	−0.44	3.33	−1.04	9.01	0.60
6	7.11	−0.92	7.23	−1.92	1.66	1.00
7	7.91	−0.78	7.69	−1.76	2.86	0.98
8	8.12	−0.74	8.15	−1.65	0.37	0.91
9	8.74	−0.80	8.62	−1.60	1.39	0.80

TABLE 2 Measurement Analysis of Strengthened Transmission Resonant Frequency and its Amplitude

Number	Frequency Prediction (GHz)	Magnitude Prediction (dB)	Frequency Measurement (GHz)	Magnitude Measurement (dB)	Frequency Relative Error (%)	Magnitude Deviation (dB)
1	1.34	−0.78	1.47	−0.43	8.84	0.35
2	1.95	−0.61	1.93	−0.50	1.04	0.11
3	2.19	−1.00	2.41	−0.56	9.13	0.45
4	2.89	−0.80	2.87	−0.65	0.70	0.14
5	3.00	−1.19	3.30	−0.80	9.09	0.39
6	7.06	−3.68	7.23	−2.60	2.35	1.09
7	7.84	−4.44	7.67	−2.53	2.22	1.92
8	8.17	−3.30	8.12	−2.60	0.62	0.71
9	8.66	−5.16	8.56	−2.80	1.17	2.35

surement analysis respectively, which are from the phase coherence prediction of one unit cell and the actual simulation/measurement of two unit cells. In both tables, the frequency prediction and magnitude prediction are obtained by Eqs. (4) and (5) with simulated or measured characteristics of one unit cell. The fourth and fifth column of the tables are from the practical simulation or measurement of two unit cells. Frequency relative error is the ratio of absolute frequency difference to the frequency simulation or frequency measurement. And the magnitude deviation is the absolute error between magnitude prediction and magnitude simulation or measurement.

As illustrated in Tables 1 and 2, the frequency relative errors are all below 10% and most of them are less than 5%. Meanwhile, the magnitude deviations are mostly within 1 dB. Both these results demonstrate the validity of the proposed method for transmission resonant frequency and its amplitude prediction. The frequency relative error is mainly caused by the error from phase simulation and measurement and the simplified model for transmission coherence analysis. The magnitude deviations from the measurement are relatively larger at high frequency due to the greater measured S-parameters error of one unit cell at these frequencies.

In fact, there should be a predicted resonant frequency around 5.04 GHz at which the phase for reflection coefficient satisfies Eq. (4) in both simulated and measured phase of one unit cell. However, this frequency is within the bandgap of microstrip EBG structure and it is very difficult to distinguish the strengthened transmission resonance phenomenon of two unit cells within the bandgap. Henceforth, this frequency is not listed in the tables.

Actually, there are more than nine strengthened resonant frequencies in the transmission coefficient of two unit cells. Some missing resonant frequencies in the phase coherence method prediction may be explained as follows. First, the unit cell used in the simulation and measurement is not a minimum repeated unit cell. Therefore, the interaction between different rectangle holes in the unit cell and two unit cells is not considered. Second, the simplified analysis model ignores the transmitted voltages produced by the multiple reflections and transmissions through the first and second unit cell. Nevertheless, these predicted resonant frequencies will provide sufficient information for the design of EBG structure.

4. CONCLUSION

A new method based on phase coherence is proposed for transmission resonant frequency and its amplitude prediction, and it is validated by the microstrip EBG structure. Both the predicted strengthened transmission resonant frequency and its amplitude agree well with the actual simulation and measurement. The proposed method has a clear physical meaning and shows great convenience for the resonant frequency prediction of multiple unit cells for EBG structure.

REFERENCES

1. V. Radisic, Y. Qian, R. Coccioli, and T. Itoh, Novel 2-D photonic bandgap structure for microstrip lines, IEEE Microwave Guided Wave Lett 8 (1998), 69–71.
2. D. Ahn, J.-S. Park, C.-S. Kim, J. Kim, Y. Qian, and T. Itoh, A design of the low-pass filter using the novel microstrip defected ground structure, IEEE Trans Microwave Theory Tech 49 (2001), 86–92.
3. G. Zhang, N. Yuan, Y. Fu, and C. Zhu, A novel PBG structure for microstrip lines, In: Microwave Millimeter Wave Technol Proceedings 3, China, 2002, pp. 1040–1042.
4. H. Kim and R. F. Drayton, Development of analysis method of electromagnetic bandgap structures to predict EBG behavior based on circuit models, In: IEEE Antennas Propagation Society International Symposium, Albuquerque, 2006, pp. 1951–1954.
5. E. Tahanian, S. Chamaani, and S.A. Mirtaheri, Compact ultra-wideband bandpass filters using EBG, Electron Lett 46 (2010), 1328–1330.
6. J. Cheng and A. Alphones, Compact interdigital microstrip band pass filter, Microwave Opt Technol Lett 52 (2010), 2128–2132.
7. H. Chu and X. Q. Shi, Ultra-wideband bandpass filter with a notch band using EBG array etched ground, Microwave Opt Technol Lett 53 (2011), 1290–1293.
8. B. Mohajer-Iravani and O.M. Ramahi, Wideband circuit model for planar EBG structures, IEEE Trans Adv Packag 33 (2010), 169–179.
9. J.W. Jewett, Jr. and R.A. Serway, University physics for scientists and engineers, Eighth ed., China Machine Press, 2010.
10. D.M. Pozar, Microwave engineering, Third ed., John Wiley, Hoboken, NJ, 2005.

A SINGLE-FED SLOT-APERTURE HYBRID ANTENNA FOR BROADBAND CIRCULAR POLARIZATION OPERATIONS

Yu-Chun Lu,[1] Ming-Je Yu,[2] and Yi-Cheng Lin[3]
[1] Graduate Institute of Communication Engineering, National Taiwan University, Taipei, Taiwan 10617, Republic of China
[2] BandRich Inc., New Taipei City, Taiwan 23145, Republic of China
[3] Department of Electrical Engineering, National Taiwan University, Taipei, Taiwan 10617, Republic of China; Corresponding author: yclin@cc.ee.ntu.edu.tw

ABSTRACT: *This article presents a microstrip-fed slot-aperture hybrid antenna for wideband circularly polarized (CP) operations. The antenna consists of a U-shaped slot, a rectangular aperture, and a probing strip fed by a microstrip line. In general, the U-shaped slot and the rectangular aperture resonate at two separate frequencies. When properly arranged, the proposed antenna may resonate over a single wideband of CP radiation. The 3-dB axial ratio (AR) bandwidth of the presented antenna in free space is about 27% with the gain level about 34 dBic. When a planar reflector is incorporated for the desirable unidirectional pattern, the presented antenna has an enhanced gain about 7 dBic with a 3-dB AR bandwidth of 25% and a front-to-back ratio of about 14 dB. Good agreement between measured and simulated results was achieved.* © 2011 Wiley Periodicals, Inc. Microwave Opt Technol Lett 54:412–415, 2012; View this article online at wileyonlinelibrary.com. DOI 10.1002/mop.26569

1. INTRODUCTION

There has been growing interest in the research on low cost and planar circularly polarized (CP) antennas. A CP antenna may mitigate multipath interferences and allow for arbitrary orientation in the alignment of polarization matching between the transmitting antenna and the receiving antenna. There have been several reported approaches to the design of CP antennas. For conventional CP patch antennas, offset feeding schemes were proposed for the generation of CP radiation [1, 2]. One can achieve CP operations also by adding extra metal parts to the patch [3] or by etching slots on the patch [4]. In Ref. 5, researchers introduced a microstrip-fed bent slot antenna with a one-and-one-half wavelength to generate combined resonant and traveling waves for CP operations. A cylindrical ring dielectric antenna of orthogonal